

SIGNAL PROCESSING FOR A LASER BASED AIR DATA SYSTEM IN COMMERCIAL AIRCRAFTS

Theodoros Katsibas¹, Theodoros Semertzidis¹, Xavier Lacondemine² and Nikos Grammalidis¹

¹Centre for Research and Technology Hellas, Informatics and Telematics Institute
1st km Thermi-Panorama road, GR-57001, Thessaloniki, Greece
phone: +30 2310464160(ext.218), fax:+30 2310464164, emails: tkatsiba@iti.gr, theosem@iti.gr, ngramm@iti.gr
web: www.iti.gr

²THALES Aerospace Division
25 Rue Jules Vedrines, 26027, Valence Cedex, France
phone: +33 4 75793610, fax: +33 4 75798655, email: xavier.lacondemine@fr.thalesgroup.com
web: www.thalesgroup.com

ABSTRACT

A systematic approach for the design and implementation of an efficient and reliable signal processing unit able to provide vital flight parameters to the cockpit of an aircraft using a properly built LIDAR equipment is presented in this paper. Taking into account the specific characteristics of a signal coming out from such an optical device we define all the necessary steps for the real-time data acquisition and processing in order to extract accurate information about the true air speed (TAS) of the aircraft and other useful flight parameters. Simulation results using properly modeled signals verified the effectiveness of the suggested methodology. The proposed scheme is being developed in the framework of the EU funded NESLIE research project and aims to be finally flight tested in order to demonstrate the availability of accurate measurements in all weather conditions and in any phase of flight.

1. INTRODUCTION

The Light Detection And Ranging (LIDAR) technique has already found great application in many fields of science such as geology, seismology, geography, atmospheric chemistry and physics as well as meteorology. Studying the light backscattering characteristics of distant targets, usually aerosol particles or molecules, one can measure numerous important parameters and perform advanced surveying and mapping tasks.

Doppler lidars specifically, utilizing the well known Doppler effect, calculate the frequency shift that moving targets may cause to the backscattered laser signal and estimate the radial component of the corresponding velocity vector. This technology constitutes a powerful tool for remote measurements of atmospheric wind fields and detailed observation of weather phenomena [1]-[3]. Starting from ground-based lidar systems, continuing advances in optics and laser industry have led to the

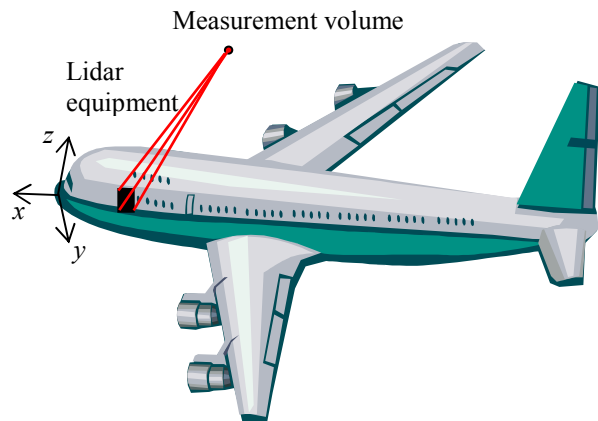


Figure 1 – On board installation of the LIDAR system

development of efficient airborne and space-based lidar units [4]. Coherent CO₂ Doppler lidar operating in NASA Marshall Space Flight Center at a wavelength of 10.6- μ m [1], [2] has been followed by the introduction of solid-state Doppler lidar, [5]-[7], and demonstrated the capability of the continuous wave system to perform single-particle detection. In addition, the fact that the Doppler shift for optical wavelengths is high enough enables us to estimate the radial velocity for each backscattered pulse [8]-[10]. Furthermore, the emergence of the eye-safe 1.5- μ m infrared laser technology that proved of great performance allowed the implementation of low cost compact optical systems. All these achievements motivated NESLIE (New Standby Lidar InstrumEnt) research project partners and an ambitious plan of developing a functional, laser based, air data standby channel has been envisaged (Figure 1). The methodology and the detailed description of all the necessary steps in the signal processing chain of such an air data system that is going to work complementary to the existing, traditional pneumatic systems constitute the objective of this paper.

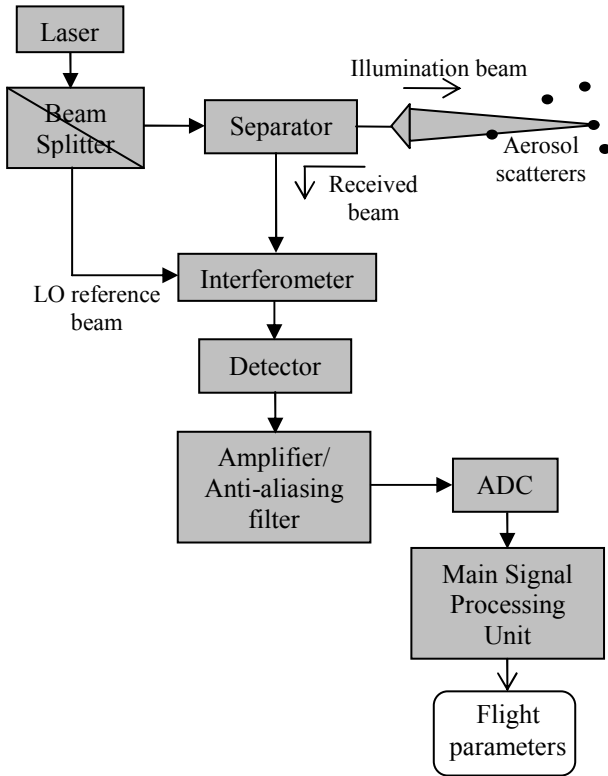


Figure 2 – The coherent single particle measurement principle

The overall measurement mechanism and the theoretical characteristics of a signal resulting from single-particle backscattering are briefly discussed in section 2.

In section 3, the proposed scheme for the consecutive processing of the acquired signal that can lead to successful real-time velocity measurements is fully presented. Two main functions are being developed: The high speed processing for frequency analysis and detection and the slow processing for 3D air-speed computation. The last paragraph concerns the definition of the appropriate hardware that can meet the system's great requirements.

2. SYSTEM'S LAYOUT AND SIGNAL CHARACTERISTICS

The general principal of the coherent single-particle Laser Doppler Anemometry is depicted in Figure 2. A continuous wave optical signal is emitted in the atmosphere and the backscattering radiation from a single, every time, aerosol particle is received. Then, the received signal and an identical copy of the emitted wave produced in a local oscillator are superimposed and feed the detector that converts the optical power into a practical electrical HF signal, containing the Doppler frequency shift information we are seeking for.

The signal processing procedure is coming next to guarantee real-time Doppler frequency detection and accurate velocity estimation. That is to provide the speed

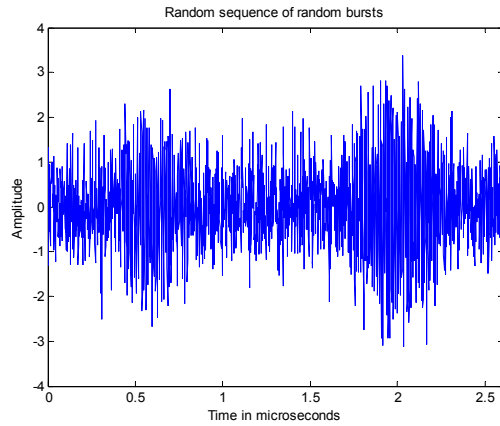


Figure 3 – Two successive modeled signal bursts buried in noise

of the aircraft relative to the air mass in which it flies projected to the laser axis. The longitudinal component of the air speed 3-D vector is given by the following equation

$$V_{long} = \frac{v_D \cdot \lambda}{2} \quad (1)$$

Where, V_{long} is the longitudinal velocity component, v_D the Doppler frequency shift and λ the wavelength of the laser. Since we aim to deliver at a constant rate the three-dimensional vector of the true air-speed, at least three identical laser units are needed to be installed on board the plane. However, one more additional unit is going to be used for better precision and control. All laser beams are focalized at the same measurement volume and at a properly chosen distance (Fig. 1). During the time a particle crosses the beam in that small volume it is illuminated with an optical power of very high density and scatters back a significant amount of energy (Fig. 2).

Resulting from such a process, the received signal is expected to be a sequence of random bursts at random time instants plus noise. Figure 3 shows two such modeled sinusoidal carriers with Gaussian envelope buried in noise. The frequency of such a burst corresponds to the value of the Doppler frequency shift and depends on the longitudinal velocity component as it has already been written (Eq. (1)). The time duration of each burst is a function of the transversal velocity component and the laser's beam diameter whereas the amplitude a function of the particle's cross-section and its characteristic trajectory crossing the laser beam. Of course, most of the time we expect to receive only noise, especially at higher flight levels where low concentration of aerosol scatterers occurs.

3. THE SIGNAL PROCESSING TASK

As already explained in section 2, the electrical HF signal constitutes the input of the signal processing (SP) unit. Before proceeding to the main SP function that

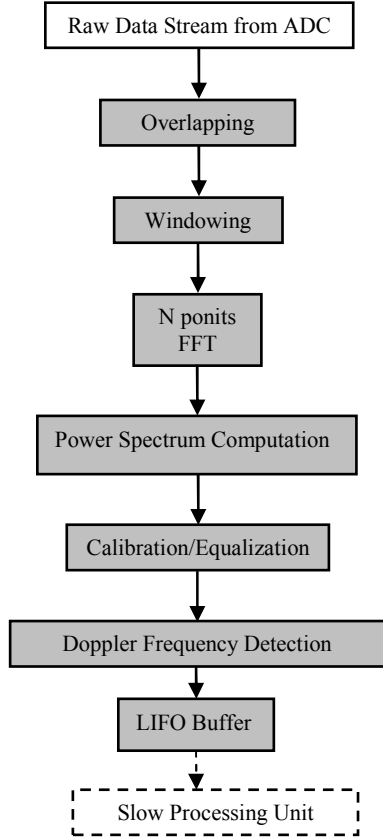


Figure 4 – The simplified high speed signal processing chain

performs the Doppler frequency detection and estimation it is necessary to amplify and low-pass filter the continuous, time-domain signal in order to eliminate the aliasing effect. That is the input signal at or above half the sampling frequency must be severely attenuated at a level below the dynamic range of the analog-to-digital (ADC) converter. The signal is then digitized in the ADC with m bits resolution. This translates to the usage of 2^m quantization levels that are going to cover the full amplitude range of the received signal. Any effort for increasing the quantization levels and further analysis does not add anything more than just measuring noise. The sampling frequency according to the Shannon-Nyquist sampling theorem should be higher than twice the highest frequency of interest. This is the maximum Doppler frequency shift that is expected to be caused to the received signal and is determined from the corresponding maximum airplane speed we wish to measure every time. As a consequence, the data samples have to be taken at a very high rate.

3.1 The fast signal processing function

The real-time application requires the fast and effective processing of a considerably high data rate. The basic successive steps of such a task are clearly shown in Figure 4.

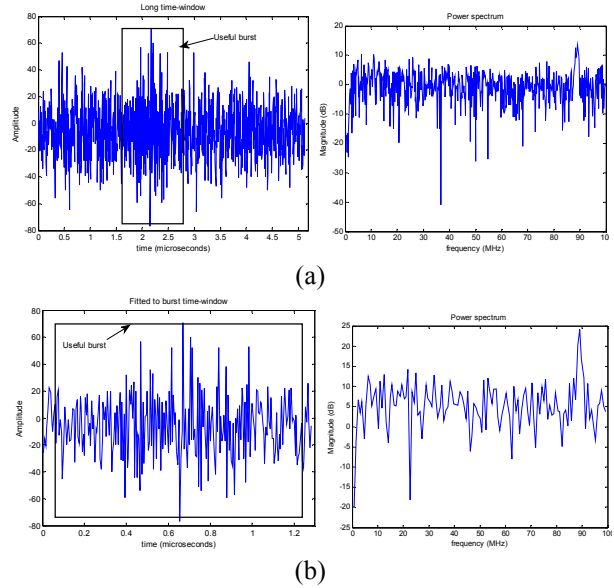


Figure 5 – Spectral analysis of a relatively long time-window containing a burst (a) and a time-window almost fitting the burst (b)

Since the whole concept relies on the Doppler effect and the exact calculation of the frequency shift caused in the received signal the Fast Fourier Transform (FFT) and the power spectrum computation and analysis constitute the powerful tools for effectively treating and processing the acquired data sequence [11], [12]. The signal data are properly time-windowed in frames of N samples and driven to the FFT block for the frequency content calculation. Despite the fact that the generated bursts are expected to be Gaussian shaped by nature it is preferred the data frames be properly weighted by a Gaussian function and not just using the rectangular window. The reason for this is that due to the appearance of the spectral leakage effect after the FFT computation of a finite in time signal the choice of the Gauss weighting window improves the obtained signal-to-noise ratio (SNR) since it is of higher dynamic range than the respective rectangular window. On the other hand, it also preserves the excellent resolution characteristics of the rectangular window and thus constitutes a good choice among other moderate window functions in an effort to reach the best trade-off between a satisfying SNR and an increased frequency resolution.

The SNR is further improved by fitting the time-window to the exact length of the shortest expected burst in an effort to ease the detection process. Figure 5(a) depicts a relatively long signal time-window containing a backscattering burst, the length of which is marked by a rectangular frame, as well as the respective power spectrum. On the other hand, Figure 5(b) shows the same burst in a time-window that almost fits its length and the corresponding power spectrum presenting a clearly improved SNR. This happens because it is just the bursts that contain all the useful information of the

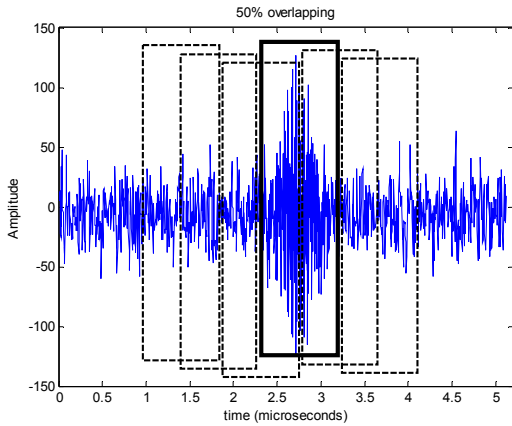


Figure 6 – Overlap processing of the data stream

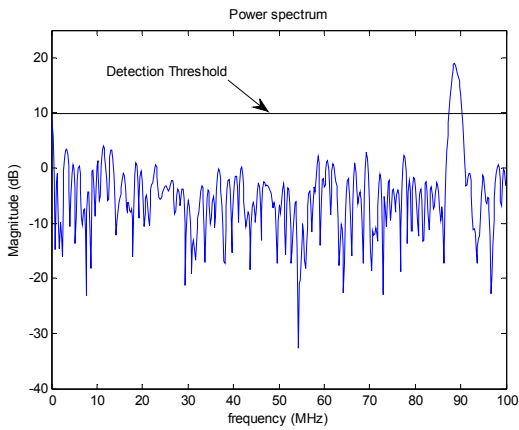


Figure 7 – Power spectrum analysis and signal detection

signal. The other parts contain pure noise and when they are subtracted from the data window the SNR is notably raised. This is, of course, at the cost of the obtained frequency resolution due to the fewer data samples used (FFT points).

The zero-padding technique may be employed to overcome that drawback by adding zeros and increasing the length of the data time-window to the desired magnitude. In this case, the detection is slightly improved due to the scalloping loss reduction and at the same time the frequency estimation is better enough, without the need for post processing.

It is also emphasized that since successive time-windows of the signal sequence are acquired and processed and the exact time a burst occurs is not previously known it is possible to lose the desired adjustment of the window to the full length of the burst if, for example, the latter happens between two successive data acquisitions. The SNR in such a case dramatically deteriorates making the detection doubtful. In order to tackle with this the overlap processing is taking place. Figure 6 illustrates the successive data windows for the 50% overlapping procedure. A serial-to-parallel conversion with adequate overlapping can fully secure the effective processing of the data sequence. In that way, a number of parallel data

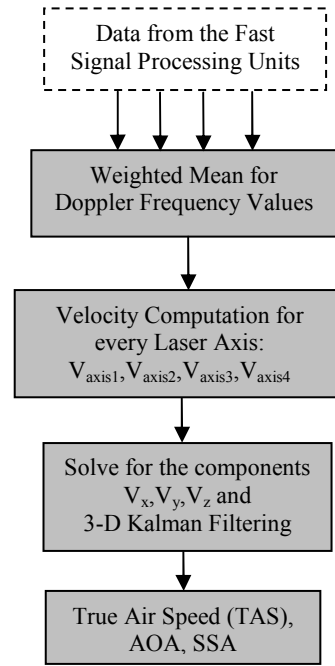


Figure 8 – The slow signal processing chain

streams are generated and processed in blocks of N samples.

Before detection, it is also necessary to calibrate the power spectrum for the bias removal and the equalization reasons. In order to calculate the calibration coefficients a spectrum is regularly acquired with the laser power set to off and the local oscillator set to on and sent to the slow processing unit.

The burst detection and the Doppler frequency estimation are then performed by spectral analysis comparing the values of the obtained power spectrum with a properly defined threshold. The power values exceeding the threshold level constitute the detected signal whereas the FFT bin of the peak value determines the corresponding Doppler frequency. Figure 7 shows the spectrum of the powerful burst depicted in Figure 6 that can provide a strong signal and an easy detection.

Finally, the detected frequencies are registered in a LIFO buffer, from where they are read in the slow processing unit for the velocity calculation.

3.2 The slow signal processing function

A schematic description of the main steps in this final stage of signal processing is given in Figure 8. The detected Doppler frequency values as well as the power values of each detected signal are collected in the CPU from the four independent laser channels. Additional parameters such as the frequency width and the power of the detected signal, which are related to the reliability of the measurement, are then estimated and used to weight the results. Since the remaining objective is to calculate the 3-D air-speed vector the frequency

measurements are accumulated for each channel and four weighted mean quantities come up. From these values, four velocities are then computed via Equation (1) corresponding to the components of the 3-D air-speed vector (\vec{V}_{TAS}) in the four laser axes. The respective velocity components V_x, V_y, V_z of \vec{V}_{TAS} in the three axes of the predefined rectangular coordinates system (Fig. 1) depend on the specific geometrical characteristics of the four measurement axes configuration and can be estimated solving a set of four equations with three unknowns. Kalman filtering may also be used in order to mitigate the noise effects and estimate the true air-speed vector at a fixed rate. Additional important flight parameters such as the angle of attack (AOA) and the side-slip angle (SSA) are also computed from TAS. A secondary task of the slow signal processing module is to perform the necessary calculation of the spectrum calibration coefficients for the bias removal and the proper adjustment of the noise level.

4. IMPLEMENTATION IN HARDWARE

The specified signal processing algorithms have to be implemented in a well suited hardware. The huge computational throughput at a considerably high clock rate and the demanding, real-time fast signal processing application necessitates the usage of powerful FPGA (field-programmable gate array) boards. Special consideration is given to the data collection time and to the processing speed of the FPGA processor which constitutes the time it takes to perform the FFT spectrum analysis and all the needed additional functions. The inherent parallelism of the logic resources in the FPGA as well as the flexibility it presents allow for high performance processing. For this purpose, the SMT700-SX95T PCI express development board based on a Xilinx Virtex 5-SX95T FPGA with more than 46,000 logic cells was chosen. This board can meet the system's advanced requirements and satisfy the strict timing constraints. The hardware platform is complemented with the SMT391 ADC board and the PCI 64 bit SMT145 carrier card.

5. CONCLUSIONS

The specifications of the efficient signal processing algorithms that may provide air-speed measurements and other useful flight parameters from a lidar signal were analytically presented. Studying the expected signal characteristics and using appropriate modelled data the proposed algorithms were extensively simulated and tested showing satisfactory results. The whole unit is being developed in the framework of NESLIE research project and planned to be flight tested in order to prove its effectiveness for on board real-time measurements.

ACKNOWLEDGMENT

This work was supported by the European Community (EC) under the FP6 Aeronautics and Space "NESLIE – NEw Standy Lidar InstrumEnt" project (Contract no.: 30721).

REFERENCES

- [1] J. Bilbro, G. Fichtl, D. Fitzjarrald and M. Krause, "Airborne Doppler lidar wind field measurements," *Bull. Am. Meteorol. Soc.* 65, pp. 348-359, 1984.
- [2] J. W. Bilbro, C. DiMarzio, D. Fitzjarrald, S. Johnson and W. Jones, "Airborne Doppler lidar measurements," *Appl. Opt.* 25, pp. 3952-3960, 1986.
- [3] M. J. Post and R. E. Cupp, "Optimizing a pulsed Doppler lidar," *Appl. Opt.* 29, pp. 4145-4158, 1990.
- [4] E.V. Browell, S. Ismail and W.B. Grant, "Differential absorption lidar (DIAL) measurements from air and space," *Appl. Phys. B* 67, pp. 399-410, 1998
- [5] M. J. Kavaya, J. R. Magee, C. P. Hale and R. M. Huffaker, "Remote wind profiling with a solid-state Nd:YAG coherent lidar system," *Opt. Lett.* 14, pp. 776-778, 1989.
- [6] S. W. Henderson, P. J. M. Suni, C. P. Hale, S. M. Hannon, J. R. Magee, D. L. Bruns and E. H. Yuen, "Coherent laser radar at 2 μm using solid state lasers," *IEEE Trans. Geosci. Remote Sens.*, 31, pp. 4-15, 1993.
- [7] R. Frehlich, S. M. Hannon and S. W. Henderson, "Performance of a 2 μm coherent Doppler lidar for wind measurements," *Journal Atm. Oc. Tech.*, vol.11, pp. 1517-1528, Dec. 1994.
- [8] M. J. Levin, "Power spectrum parameter estimation," *IEEE Trans. Inform. Theory*, vol. 11, pp. 100-107, Jan. 1965.
- [9] P. R. Mahapatra and D. S. Zrnic, "Practical algorithms for mean velocity estimation in pulse Doppler weather radars using a small number of samples," *IEEE Trans. Geosci. Remote Sens.*, vol. GE-21, No 4, pp. 491-501, Oct. 1983.
- [10] R. G. Frehlich and M. J. Yadlowsky, "Performance of mean-frequency estimators for Doppler radar and lidar," *Journal Atm. Oc. Tech.*, vol.11, pp. 1217-1229, Oct. 1994.
- [11] J. G. Proakis and D. K. Manolakis, *Digital Signal Processing*. Prentice Hall (forth edition), 2006.
- [12] A. V. Oppenheim and R. W. Schaffer, *Discrete-Time Signal Processing*. Prentice Hall, 1999.